Journal of Pharmaceutical and Biomedical Analysis 55 (2011) 366–372

Contents lists available at ScienceDirect

Journal of Pharmaceutical and Biomedical Analysis

journal homepage: www.elsevier.com/locate/jpba

Short communication

Isolation and identification of five impurities of ALB 109564(a) drug substance

Dennis J. Milanowski[a], Jeff Keilman[a], Cheng Guo[b], Ulla Mocek[a,*]

[a] AMRI, Bothell Research Center, 22215 26th Ave. SE, Bothell, WA 98021, United States
[b] AMRI, 26 Corporate Circle, P.O. Box 15098, Albany, NY 12212-5098, United States

ARTICLE INFO

Article history:
Received 17 November 2010
Received in revised form 21 January 2011
Accepted 26 January 2011
Available online 3 February 2011

Keywords:
ALB 109564(a)
Tubulin inhibitor
Impurities
Structure elucidation
Capillary NMR

ABSTRACT

Four low-level impurities were detected during the development and scale up of the synthesis of ALB 109564(a). These impurities were isolated and characterized in order to determine how they originated in the drug substance. The information allowed the elimination of one impurity and a significant reduction in the relative abundance of the other three. A fifth impurity was detected in an accelerated stability study sample of the drug substance. The degradant was found to be the free acid resulting from the hydrolysis of the methyl ester within the indoline moiety of ALB 109564(a). The characterization of this impurity allowed for changes in the handling of the drug substance which minimized the formation of the impurity.

© 2011 Elsevier B.V. All rights reserved.

1. Introduction

ALB 109564(a) (**1**·2HCl, Fig. 1) is a novel analog within an established class of tubulin inhibitors structurally related to vinblastine [1–3] that is currently in phase I clinical trials. ALB 109564(a) is a cytotoxic agent designed to kill cancer cells by disrupting mitosis [4–6] and has demonstrated improved efficacy over marketed members of its class in preclinical testing.

The International Conference on Harmonization (ICH) sets standards for the purity of drug substances [7]. Since ALB 109564(a) is to be given at levels of <2 g/day, the guidance states that impurities present at levels between 0.10% and 0.15% should be identified. Impurities present at levels ≥0.15% must be qualified according to the ICH standards. Four previously uncharacterized impurities (**2**–**5**) were observed in the drug substance at 0.5–0.7% using the cGMP chemical process to produce material for clinical testing. Three of the impurities (**2**–**4**) were present in the material used in the investigational new drug (IND) enabling safety studies, and thus qualified at those levels. The fourth impurity (**5**) was a new impurity and thus not qualified (Table 1). It was determined that compliance with the ICH guidance, even at this early stage of development, was desirable. Consequently, isolation and structural characterization of these impurities was critical to guide synthetic and handling modifications to reduce or eliminate the formation of the impurities.

Subsequent to the identification of impurities **2**–**5** in the drug substance, a sample of ALB 109564(a) from a stability study showed the presence of a degradant (**6**), which did not correspond to any of the previously identified impurities. Isolation and structural characterization of the degradant was undertaken to minimize the formation of this degradant in the drug product.

The isolation and structural characterization of four impurities and a degradant of ALB 109564(a) drug substance are reported in this paper. We have developed a rapid protocol, used routinely for the isolation and characterization of trace impurities in drug substances and formulated drug products, which was employed in the characterization of **2**–**6**. The strategy utilizes a combination of spectrometric and spectroscopic techniques to analyze impurities during and after isolation, minimizing the analysis time. The recent application of capillary NMR (CapNMR) has facilitated this by reducing the amount of an impurity that must be isolated to allow acquisition of NMR data which is traditionally the technique requiring the most sample.

2. Experimental

2.1. Materials

ALB 109564(a) drug substance and vinblastine sulfate were generated at AMRI. Acetonitrile (HPLC grade) was purchased from Fisher Scientific. Purified water was obtained from a Millipore Milli-Q Plus system (Bedford, MA). Spectrophotometric grade trifluoroacetic acid (TFA) was purchased from Sigma–Aldrich. CD_3OD and TFA-*d* were obtained from Cambridge Isotopes.

* Corresponding author. Tel.: +1 425 686 6875; fax: +1 425 686 6799.
E-mail address: ulla.mocek@amriglobal.com (U. Mocek).

0731-7085/$ – see front matter © 2011 Elsevier B.V. All rights reserved.
doi:10.1016/j.jpba.2011.01.035

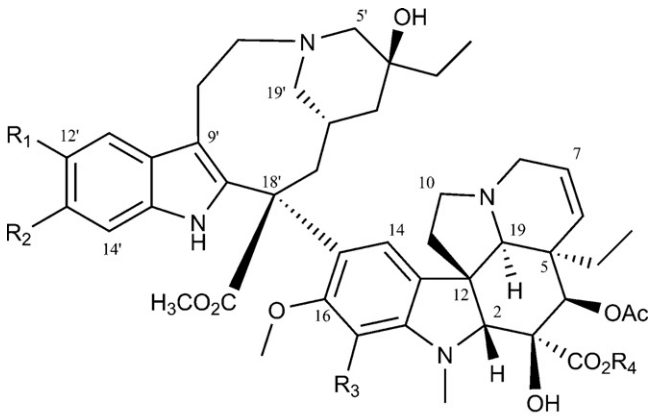

	R_1	R_2	R_3	R_4
1	SCH_3	H	H	CH_3
2	H	H	H	CH_3
3	H	SCH_3	H	CH_3
4	SCH_3	H	Br	CH_3
5	SCH_3	H	I	CH_3
6	SCH_3	H	H	H

Fig. 1. Structures of compounds **1**–**6**.

2.2. Stability sample

Samples of ALB 109564(a) were stored at −20 °C, 5 °C and 25 °C/60% relative humidity (RH) in amber glass bottles with Teflon-lined screw caps, under a layer of nitrogen. The sample design called for the periodic analysis of samples over 12 months. During the course of the stability study, the relative abundance of a degradant eluting at relative retention time (RRT) 0.79 (**6**) was observed to increase. Stability samples from the 5 month time point were utilized for the isolation of **6**.

2.3. High performance liquid chromatography (HPLC) and isolations

Semi-preparative HPLC was carried out using a Waters 600E pump connected to a Waters 996 diode-array detector and controlled by Waters Empower software. The isolation utilized a Phenomenex Luna C_{18} column (250 mm × 10 mm, 5 μm, p/n 00G-4252-N0) under ambient conditions at a flow rate of 5 mL/min. Mobile phases A and B consisted of H_2O (0.1% TFA) and acetonitrile (0.1% TFA), respectively. A linear gradient was used increasing from 30% to 45% B over the first 19 min and increasing to 90% B over an additional 5 min.

Table 1
Relative abundance of **2**–**6** in ALB 109564(a) lots.

Compound	ALB 109564(a) Lot	
	Qualification/Tox Lot	Development Lot
2	0.11%	0.53%
3	0.64%	0.60%
4	0.65%	0.69%
5	ND[a]	0.69%
6	0.19%	0.04%

[a] ND = not detected.

Isolations of **2**, **4** and **5** were carried out using a sample of the ALB 109564(a) drug substance that was prepared at 100 mg/mL in H_2O and the separation was monitored at 220 nm. A sample of **2** was isolated from a single 80 μL (8 mg) injection. The fraction containing **2** (16.1 min) was collected and concentrated under a stream of N_2. Separately, a total of 150 mg was separated over the course of 6 injections of 200–400 μL (20–40 mg) to provide a crude fraction containing **4** and **5**. The crude impurity fraction was taken up in 1.2 mL of H_2O–methanol (5:1) and separated over 6 injections utilizing an isocratic method consisting of 38% mobile phase B. The fractions containing **4** (9.54 min) and **5** (10.24 min) were collected separately, pooled, and concentrated under a stream of N_2.

The semi-preparative HPLC method described above was also utilized to isolate **6**. An aliquot of the ALB 109564(a) stability sample was prepared at 100 mg/mL in H_2O and separated over the course of multiple 20–40 μL injections (2–4 mg each). The fraction containing **6** (10.61 min) was collected, pooled, and concentrated under a stream of N_2. The sample used for acquisition of NMR data using the CapNMR probe was obtained from a single 40 μL (4 mg) injection of the stability sample.

The limited resolution observed between **1** and **3** required the development of a modified method for isolation and restricted the amount of **3** which was isolated. Impurity **3** was purified in a two-step process. The isolation of **3** utilized a modified semi-preparative method employing the same column, flow rate and mobile phases used above. A sample of the drug substance was prepared at 10 mg/mL in H_2O and the injection volume was 100 μL (1 mg). A total of 7 mg of the drug substance was separated over 7 injections utilizing an isocratic method consisting of 27% mobile phase B. Impurity **3** eluted with the leading edge of the broad peak containing **1**. The leading edge of the drug substance peak (22–25 min), including **3**, was collected as the crude impurity fraction. This fraction was taken up in 200 μL of H_2O and separated using the analytical method described in the LC–MS section below, except that all of the eluent exiting the column was directed through the DAD. The peak containing **3** eluted at 11.32 min and was collected and dried under a stream of N_2.

2.4. LC–MS

Samples were analyzed using a Sciex API150 MCA system incorporating an Agilent 1100 LC pump connected to an Agilent 1100 DAD and Sciex API150 single quadrupole mass analyzer. Analysis of the samples was performed using the following method: column: Intakt Cadenza C_{18}, 4.6 mm × 150 mm, 3 μm (p/n CD005); mobile phase A: H_2O (0.1% TFA); mobile phase B: acetonitrile (0.1% TFA); flow rate: 1.0 mL/min; column temperature: 40 °C; injection volume: 50 μL. A linear gradient was employed increasing from 30% to 45% B over the first 19 min and then increasing to 90% B over an additional 5 min. The eluent was split post-column and ca. 90% was directed into the DAD monitoring at 215 nm with the remainder introduced into the mass analyzer via positive atmospheric pressure chemical ionization (APCI+) using a heated nebulizer source and scanning between *m/z* 100 and 1200.

2.5. NMR spectroscopy

NMR spectra were acquired at ambient temperature (300 K) on a Bruker Avance DRX 500 instrument operating at 500 MHz for ^1H and 125 MHz for ^{13}C. NMR data for **1** and vinblastine sulfate were acquired using a 5 mm multinuclear inverse probe with a *Z*-gradient; NMR data for the isolated compounds were acquired using either the 5 mm probe with a Shigemi tube (**4** and **5**) or an MRM/Protasis capillary NMR (CapNMR) probe with a 10 μL flow cell (**2**, **3**, and **6**). Data were acquired in CD_3OD except for

6 which were acquired in CD_3OD + 5% TFA-*d*. The spectra were referenced to the residual solvent signal (δ_H 3.30, δ_C 49.0 for CD_3OD).

2.6. Electrospray ionization (ESI)-MS

MS and MS/MS data were generated with a Waters Premier QTOF mass spectrometer equipped with an electrospray ionization source operated in positive mode. Standards or isolated compounds were diluted with H_2O–acetonitrile (1:1) containing 0.1% formic acid and infused using the onboard syringe pump. Accurate mass data were obtained in Lockspray mode using leucine enkephalin as the reference standard.

3. Results and discussion

Analytical HPLC analysis of a sample of ALB 109564(a) drug substance indicated the presence of four unknown impurities above 0.15% relative abundance. Three of the impurities (**2**–**4**) were observed in the material used for IND enabling studies and thus qualified at the levels observed. The fourth impurity (**5**) had not been observed previously. The identification of these impurities was desirable as a first step in the production of material with reduced impurity content.

The analytical HPLC method was suitable for use with LC–MS without modification. A typical UV (215 nm) chromatogram for the drug substance showing ALB 109564 (**1**) and the four impurities of interest (**2**–**5**) is provided in the top panel of Fig. 2. Analysis of the mass spectra for **1**–**5** provided a structural candidate for **2**, but only possible molecular formulas for impurities **3**–**5** which necessitated isolation of these impurities to allow further structural characterization.

3.1. Structural confirmation of impurity *2*

The earliest eluting of the impurities, **2**, showed an $[M+H]^+$ ion at *m/z* 811, suggesting that it was likely vinblastine, which differs from **1** only in that it lacks the *S*-methyl group at C-12′. The UV chromatogram for an injection of an authentic standard of vinblastine (Fig. 2, middle panel) showed the same retention time as **2**. A small sample was isolated for comparative analysis by MS and NMR. The mass of the $[M+H]^+$ ion was observed at *m/z* 811.4307, which was in good agreement with the molecular formula $C_{46}H_{58}N_4O_9$ (calcd for $C_{46}H_{59}N_4O_9$: 811.4282, error: 3.1 ppm) and confirmed that **2** has the same molecular formula as vinblastine. Final structural confirmation was made by comparison of the ^1H NMR and ^1H–^1H COSY spectra of vinblastine and the isolated sample of **2**.

3.2. Structure elucidation of impurity *3*

The mass spectrum of **3** showed an $[M+H]^+$ ion at *m/z* 811, indicating that it was an isomer of **1**. The $[M+H]^+$ ion of **3** was observed at *m/z* 857.4191, which was in good agreement with the molecular formula $C_{47}H_{60}N_4O_9S$ (calcd for $C_{47}H_{61}N_4O_9S$: 857.4159, error: 3.7 ppm) and confirmed that **3** has the same molecular formula as **1**. The MS/MS spectrum for **3** was found to be identical to that observed for **1** and so was not of assistance in assigning the structure of the impurity.

The isolated sample of **3** was taken up in 20 μL of CD_3OD and ^1H NMR and ^1H–^1H COSY spectra were acquired by CapNMR. A complete assignment of the ^1H chemical shifts for **3** was made in comparison with data acquired for **1**, **2**, and the literature data for **2** [8–11]. The data are summarized in Table 2. The NMR data for **3** indicated that the only significant differences between **1** and **3** were confined to the aromatic protons of the indole moiety (H-11′ through H-14′). Both compounds showed the presence of two doublets and a singlet attributable to the indole moiety. The splitting pattern indicated that the *S*-methyl group must be attached at either C-12′ or C-13′ for both. Since the *S*-methyl group is present at C-12′ in **1**, the data indicated that the *S*-methyl group must be at C-13′ for **3** which was supported by an analysis of the ^1H chemical shifts. H-11′ appeared as a singlet (δ_H 7.53) in **1**, but was observed as a doublet for both **2** (δ_H 7.49) and **3** (δ_H 7.42), indicative of a lack of substitution at C-12′ for **2** and **3**. For **1**–**3**, H-11′ was observed as the most downfield resonance in the ^1H NMR spectrum. A COSY correlation was observed between H-11′ and the doublet at δ_H 7.02, allowing assignment of the latter as H-12′ in **3**. Therefore, the *S*-methyl group must be present at C-13′ in **3**, and the remaining aromatic singlet observed at δ_H 7.25 can be assigned as H-14′.

3.3. Structure elucidation of impurities *4* and *5*

The mass difference observed between **4** and **1** (78 Daltons) together with the isotope pattern for the $[M+H]^+$ ion of **4**, which showed peaks at *m/z* 935 and 937 (1:1) ion, suggested the presence of a bromine substituent. Similarly, the mass difference between **5** and **1** (126 Daltons) indicated the possible presence of an iodine substituent. The $[M+H]^+$ ion of **4** was observed at *m/z* 935.3254 and was in good agreement with the molecular formula $C_{47}H_{59}BrN_4O_9S$ (calcd for $C_{47}H_{60}BrN_4O_9S$: 935.3264, error: −1.1 ppm). This data confirmed that **4** is related to **1** by substitution of a hydrogen with bromine. The MS/MS spectrum of **4** showed a fragment ion at *m/z* 399.1754, which corresponded to a fragment ion observed in the MS/MS spectrum of **1** (Fig. 3). The molecular formula for this ion, determined from the accurate mass, was found to be $C_{22}H_{27}N_2O_3S$ (calcd for $C_{22}H_{27}N_2O_3S$: 399.1742, error: 3.0 ppm) indicating that this fragment corresponded to the indole monomer (C-1′ through C-19′), which included the *S*-methyl substituent. The assignment of this fragment as the indole monomer was confirmed by the observation of a fragment ion at *m/z* 353.1891 in the MS/MS spectrum of vinblastine (**2**), which lacks the *S*-methyl substituent at C-12′. The observation that the molecular formula for the indole moiety of **1** and **4** is identical in turn indicated that the bromine must be located within the indoline moiety (N-1 through C-19) of **4**.

A comparison of the ^1H NMR spectrum acquired for **4** with that of **1** indicated that the aromatic proton present at δ_H 6.40 and corresponding to H-17 was absent in the ^1H NMR spectrum of the impurity. A complete assignment of the ^1H chemical shifts for **4** confirmed that the structure of this impurity and **1** differ only at C-17 and allowed **4** to be assigned as the 17-bromo analog of **1** (Table 1).

A similar analysis for impurity **5** indicated that it was the 17-iodo analog of **1**. The $[M+H]^+$ ion of **5** was observed at *m/z* 983.3146 and was in good agreement with the molecular formula $C_{47}H_{59}IN_4O_9S$ (calcd for $C_{47}H_{60}IN_4O_9S$: 983.3126, error: 2.0 ppm). The MS/MS spectrum of **5** showed a fragment ion at *m/z* 399.1762, confirming that the iodine substituent must be located within the indoline moiety. As was observed for **4**, the ^1H NMR spectrum of **5** lacked a signal for H-17 at δ_H 6.40 confirming that **5** is the 17-iodo analog of **1**.

Impurity **4** was synthesized by chemical methods (Fig. 4) to further confirm the structure of **4** and to provide reference standards for future studies. Direct bromination on **1** or its precursor under various conditions led to predominantly 11′-bromo or 14′-bromo byproduct. This selectivity issue was solved by deactivation of the upper aromatic ring system after turning the electron-donating methylthio group in **1** into an electron-withdrawing sulfoxide in **7** via oxidation. The reduction of the sulfoxide group back to methylthio also faced selectivity issues since the ester functionality present within several locations of the molecule is sensitive to reducing agents. After several attempts employing different reagents, the method reported by Guindon et al. turned out to be

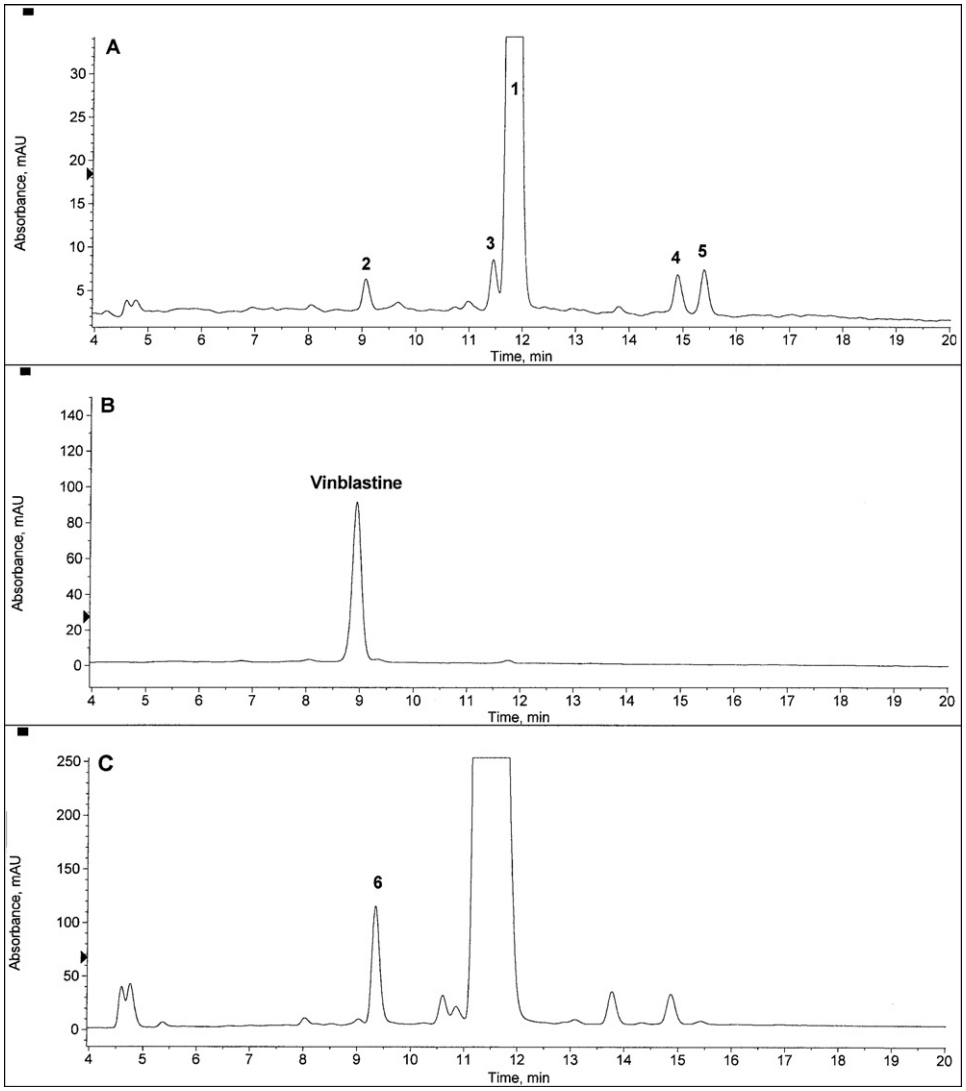

Fig. 2. (A) Typical HPLC (UV, 215 nm) impurity profile for ALB109564(a) showing ALB109564 (**1**) and impurities **2**–**5**. (B) HPLC chromatogram for vinblastine sulfate. (C) Typical HPLC degradant profile for ALB109564(a) stability sample showing degradant **6**.

effective [12]. The spectral data of synthesized **4** were fully consistent with the isolated material.

3.4. Structure elucidation of degradant *6*

Subsequent to the completion of the isolation and characterization of impurities **2**–**5**, a degradant, **6**, was observed in a stability study sample of the drug substance that did not correspond to a known impurity (Fig. 2C). LC–MS analysis of this sample showed that the new degradant eluted near impurity **2** (vinblastine), but the mass spectrum revealed an $[M+H]^+$ ion at *m/z* 843 clearly indicating that it did not correspond to **2**. The molecular formula of **6** was determined by accurate mass analysis of the isolated sample of the degradant. The $[M+H]^+$ ion of **6** was observed at *m/z* 843.4014 and was in good agreement with the molecular formula $C_{46}H_{58}N_4O_9S$ (calcd for $C_{46}H_{58}N_4O_9S$: 843.4003, error: 1.3 ppm). This data indicated that the degradant differed from **1** by the loss of a methyl group. The MS/MS spectrum of **6** showed a fragment ion at *m/z* 399.1765 indicating that the methyl loss must have occurred in the indoline moiety (N-1 through C-19) of the degradant (Fig. 5). The fragmentation pattern observed for the higher mass ions was more complex than that observed for **1** or the other impurities (**2**–**5**). Fragment ions were observed for both the loss of acetic acid (*m/z* 783.3807) and formic acid (*m/z* 797.3951), the latter corresponding to a fragment ion observed for **1** and attributed to the loss of acetic acid from the $[M+H]^+$ ion of **1**. These observations suggested that the methyl was lost from the ester at either C-3 or C-18′. Taking into account the fragment ion at *m/z* 399.1765 in both the spectra of **1** and **6**, the data suggested that the methyl loss occurred from the ester at C-3 within the indoline moiety.

A sample was isolated from 4 mg of the stability sample for acquisition of NMR data by CapNMR to confirm that the only change in the structure of the degradant was the loss of a methyl group at the C-3 ester. A comparison of the ^{1}H NMR spectra for **6** and **1** indicated that the methyl singlet observed at δ_H 3.80 in the ^{1}H NMR spectrum of **1**, which corresponded to the methyl ester at C-3, was absent in the spectrum acquired for the degradant. A complete assignment of the ^{1}H chemical shifts for the degradant confirmed that the structure of **6** differed from that of **1** only at C-3 (Table 1). The presence of a free acid in the structure of the degradant was further supported by the observation of peak doubling when the NMR data was initially acquired in CD_3OD which was resolved by the addition of a small amount of TFA-*d* to the sample prior to acquisition of NMR data.

Table 2
^{1}H NMR chemical shift assignments (500 MHz, CD_3OD) for **1**–**6**.

Position	**1**	**2**	**3**	**4**	**5**	**6**[a]
1′	2.43 m	2.44 m	2.47 m	2.23 m	2.18 m	2.48 m
	3.92 m	3.95 m	3.94 m	4.10 t (14.4)	4.11 t (14.4)	3.92 m
2′	1.38 m	1.25 m	1.37 m	1.42 m	1.46 m	1.37 m
3′	1.65 m	1.60 m	1.65 m	1.69 m	1.70 m	1.65 m
4′-CH_2CH_3	1.52 q (7.4)	1.46 q (7.4)	1.54 m	1.53 q (7.4)	1.53 q (7.4)	1.51 q (7.4)
4′-CH_2CH_3	0.96 t (7.8)	0.95 t (7.4)	0.96 t (7.4)	0.97 t (7.4)	0.97 t (7.4)	0.96 t (7.4)
5′	3.15 s	3.08 s	3.17 m	3.20 s	3.20 s	3.17 s
7′	3.63 m	3.54 m	3.63 m	3.63 m	3.65 m	3.64 m
		3.57 m				
8′	3.31 m	3.27 m	3.32 m	3.34 m	3.33 m	3.31 m
	4.63 ddd (3.0, 10.0, 17.8)	4.45 dd (10.4, 16.3)	4.62 m	4.60 m	4.58 m	4.64 m
11′	7.53 bs	7.49 d (8.2)	7.42 d (8.5)	7.53 s	7.53 s	7.52 bs
12′	–	7.05 t (7.8)	7.02 d (8.5)	–	–	–
13′	7.16 dd (1.5, 8.5)	7.11 t (7.8)	–	7.17 dd (1.5, 8.5)	7.16 d (8.5)	7.16 dd (1.5, 8.5)
14′	7.23 d (8.5)	7.21 d (8.2)	7.25 s	7.24 d (8.5)	7.23 d (8.5)	7.23 d (8.5)
18′-OMe	3.68 s	3.67 s	3.69 s	3.69 s	3.68 s	3.68 s
19′	2.86 dd (6.3, 14.4)	2.74 m	2.87 m	2.96 dd (5.9, 14.4)	2.99 m	2.85 m
	3.90 m	3.78 m	3.90 m	3.91 m	3.95 m	3.93 m
NMe	2.77 s	2.71 s	2.77 s	3.04 s	3.02 s	2.87 s
2	3.71 s	3.58 s	3.72 s	3.75 s	3.75 s	3.76 s
3-OMe	3.80 s	3.76 s	3.81 s	3.81 s	3.82 s	
4	5.34 s	5.34 s	5.34 s	5.24 s	5.23 s	5.35 s
4-OMe	2.06 s	2.02 s	2.07 s	2.07 s	2.07 s	2.06 s
5-CH_2CH_3	1.56 m	1.40 m	1.59 m	1.39 m	1.37 m	1.54 m
	1.72 m	1.67 m	1.78 m	1.67 m	1.63 m	1.76 m
5-CH_2CH_3	0.77 t (7.4)	0.77 t (7.4)	0.82 t (7.4)	0.73 t (7.4)	0.69 t (7.4)	0.79 t (7.4)
6	5.63 d (10.4)	5.30 d (10.4)	5.67 d (10.0)	5.64 d (10.4)	5.60 m	5.63 d (10.4)
7	5.93 ddd (~1, 5.2, 10.4)	5.85 dd (4.4, 10.0)	5.94 m	5.92 dd (5.2, 10.4)	5.91 dd (5.2, 10.4)	5.92 dd (4.8, 10.4)
8	3.42 d (15.0)	2.77 m	3.51 m	3.35 m	3.28 m	3.49 d (15.2)
	3.87 m	3.33 m	3.94 m	3.82 m	3.75 m	3.92 m
10	3.21 m	3.23 m	3.24 m	3.13 m	3.05 m	3.25 m
	3.70 m	3.45 m	3.79 m	3.71 m	3.65 m	3.75 m
11	2.03 m	1.85 m	2.06 m	2.02 m	1.98 m	2.04 m
	2.31 ddd (5.6, 8.9, 14.0)	2.07 m	2.34 m	2.37 m	2.33 m	2.32 m
14	6.66 s	6.53 s	6.69 s	6.70 s	6.72 s	6.68 s
16-OMe	3.85 s	3.83 s	3.85 s	3.96 s	3.93 s	3.84 s
17	6.40 s	6.34 s	6.41 s	–	–	6.38 s
19	3.70 m	3.88 s		3.67 m	3.96 m	3.69 m
S-Me	2.44 s	–	2.42 s	2.44 s	2.43 s	2.43 s

[a] Acquired in CD_3OD with 5% TFA-*d*.

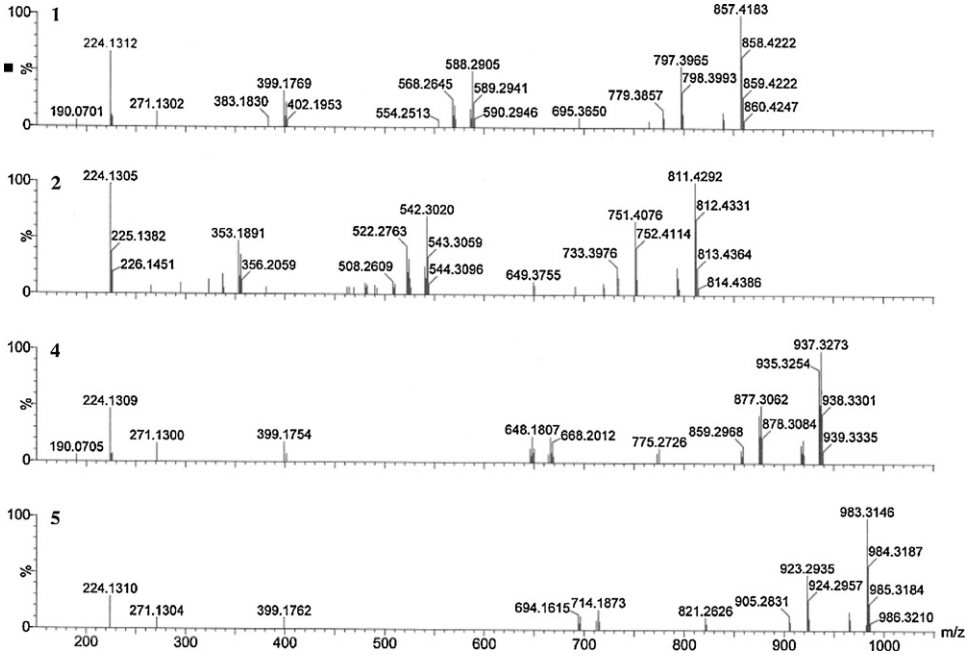

Fig. 3. MS/MS spectra of compounds **1**, **2**, **4**, and **5** selecting the $[M+H]^+$ ion for fragmentation.

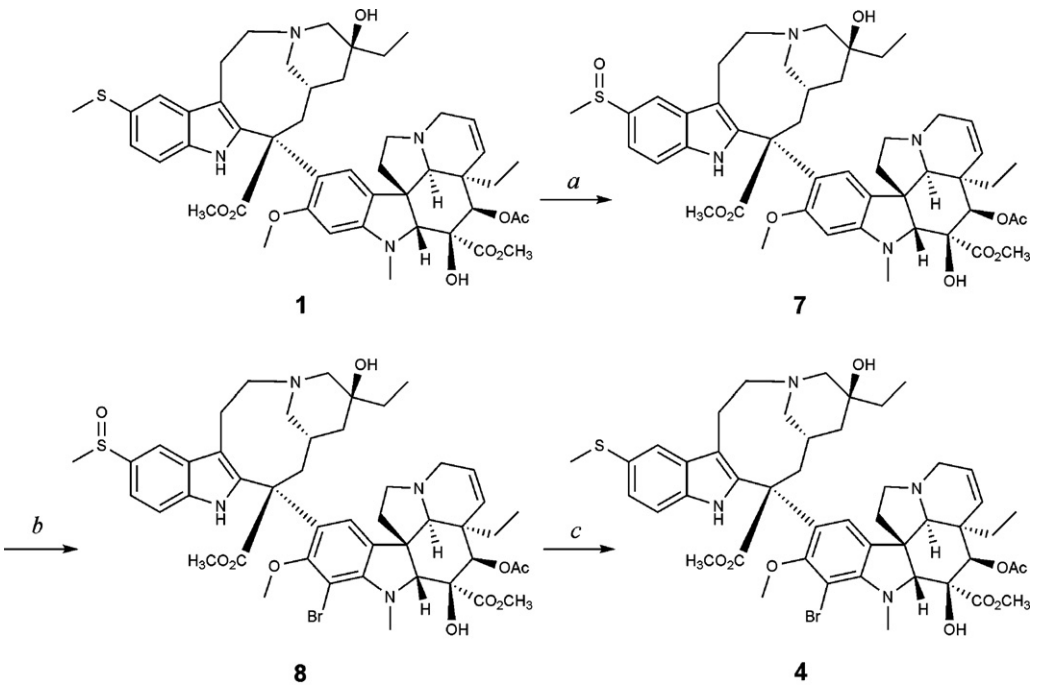

a. H_2O_2, HOAc/H_2O, 0 °C to rt, 94%; b. NBS, conc. H_2SO_4, CH_3CN, -10 °C, 97%;
c. Me_2BBr, propene, CH_2Cl_2, -20 °C to 0 °C, 68%.

Fig. 4. Synthesis of **4**.

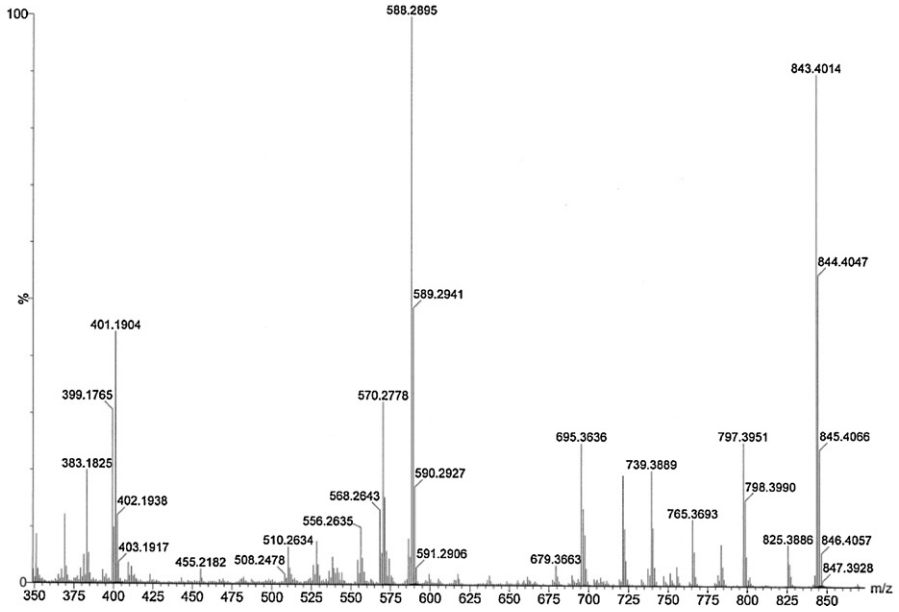

Fig. 5. MS/MS spectrum of degradant 6 selecting the $[M+H]^+$ ion for fragmentation.

The structure of **6** was also confirmed by synthesis. The hydrolysis of the ester at C-3 offered another challenge of selectivity as there are two other ester groups at C-18, and C-4 positions in **1**. The selectivity was achieved by reaction of **1** with lithium chloride in pyridine under microwave irradiation at 140 °C to provide **6** in 41% yield. Again, the spectral data of the synthetic and isolated materials were identical.

4. Conclusions

Four impurities arising during the synthesis of ALB 109564(a) were characterized and identified as compounds **2**–**5**. Impurities **3**–**5** were determined to form as a result of impurities in the initial reaction of the process. This information allowed the team to focus on ways to improve the synthesis and purification of ALB

109564(a). These efforts were successful in eliminating the formation of impurity **4** and reducing the formation of impurity **5** to <0.10%. The remaining impurities (**2** and **3**) were minimized to levels that were less than half the qualified levels of these impurities. An additional impurity was observed during stability testing of the drug substance which was identified as **6**. This degradant was eliminated by changes to the final salt form of the compound.

Acknowledgments

We would like to thank Mark Mortensen and Paul Bruzinski (AMRI, Chemical Development), Kristin Schmitz and Nicole Malinowski (AMRI, Pharmaceutical Services), Paul Brodfuehrer (AMRI, Project Management), and Regis Turske (AMRI, Manufacturing) for providing the samples as well as preliminary analytical data. Special thanks to Mark Wolf (AMRI, Medicinal Chemistry) for his guidance throughout the project and his help with the preparation of the manuscript.

References

[1] N. Neuss, M. Gorman, W. Hargrove, N.J. Cone, K. Biemann, G. Buchi, R.E. Manning, Vinca alkaloids. XXI. The structures of the oncolytic alkaloids vinblastine (VLB) and vincristine (VCR), J. Am. Chem. Soc. 86 (1964) 1440–1442.
[2] J.W. Moncrief, W.N. Lipscomb, Structures of leurocristine (vincristine) and vincaleukoblastine, J. Am. Chem. Soc. 87 (1965) 4963–4964.
[3] J.W. Moncrief, W.N. Lipscomb, Structure of leurocristine methiodide dihydrate by anomalous scattering methods: relation to leurocristine (vincristine) and vincaleukoblastine (vinblastine), Acta Crystallogr. 21 (1965) 322–331.
[4] M.E. Voss, J.M. Ralph, D. Xie, D.D. Manning, X. Chen, A.J. Frank, A.J. Leyhane, L. Liu, J.M. Stevens, C. Budde, M.D. Surman, T. Friedrich, D. Peace, I.L. Scott, M. Wolf, R. Johnson, Synthesis and SAR of vinca alkaloid analogues, Bioorg. Med. Chem. Lett. 19 (2009) 1245–1249.
[5] R.J. Owellen, C.A. Hartke, R.M. Dickerson, F.O. Hains, Inhibition of tubulin-microtubule polymerization by drugs of the vinca alkaloid class, Cancer Res. 36 (1976) 1499–1502.
[6] L. Wilson, K.M. Creswell, D. Chin, The mechanism of action of vinblastine. Binding of [acetyl-^{3}H]vinblastine to embryonic chick brain tubulin and tubulin from sea urchin sperm tail outer doublet microtubules, Biochemistry 14 (1975) 5586–5592.
[7] International Conference on Harmonization (ICH), Guidelines for Industry, Q3A, Impurities in New Drug Substances (Revision 2), June 2008.
[8] A. De Bruyn, L. De Taeye, M.J.O. Anteunis, A proton NMR study of vinblastine, Bull. Soc. Chim. Belg. 89 (1980) 629–636.
[9] P. Pfaendler, G. Bodenhausen, Analysis of multiplets in two-dimensional NMR spectra by topological classification: applications to vinblastine and cyclosporin A, Magn. Reson. Chem. 26 (1988) 888–894.
[10] J. Sapi, L. Szabo, E. Baitz-Gacs, G. Kalaus, C. Szantay, Synthesis of vinca alkaloids and related compounds XLII: transformation of vincamone into vincamines via diazomethane assisted homologization. Application of ^{1}H NOE measurements for the configurational assignment of the spirooxirane ring, Tetrahedron 44 (1988) 4619–4629.
[11] E. Gaggelli, G. Valensin, N.J. Stolowich, H.J. Williams, A.I. Scott, Conformation of vinblastine in aqueous solution determined by 2D ^{1}H- and ^{13}C-NMR spectroscopy, J. Nat. Prod. 55 (1992) 285–293.
[12] Y. Guindon, J.G. Atkinson, H.E. Morton, Deoxygenation of sulfoxides with boron bromide reagents, J. Org. Chem. 49 (1984) 4538–4540.